

Far infrared properties of PLZT ceramics

P. M. NIKOLIĆ, B. D. STOJANOVIĆ, S. DURIĆ, D. VASILJEVIĆ RADOVIĆ
Joint Laboratory for Advanced Materials of SASA, 11 000 Belgrade, P.O. Box 745, Yugoslavia

D. SIAPKAS, T. T. ZORBA
Department of Physics, Aristoteles University of Thessaloniki, 54 006 Greece

Far infrared and mid infrared reflectivity measurements have been made of lead titanate zirconate (PLZT) ceramics at room temperature in the frequency range 40–1500 cm^{-1} . Kramers–Krönig analysis and a fitting procedure based on a four parameter model of the spectrum, determined the infrared active transverse and longitudinal optical modes and their damping factors. Group theory analysis has been done and the number of experimentally observed infrared active modes was compared with the theoretical prediction. Three ionic oscillators for a cubic perovskite P_m3_m structure should exist, but four ionic oscillators for the PLZT polycrystalline sample were observed. This excluded the possibility that the sample could have a cubic lattice and confirmed that the tetragonal structure was present at room temperature. X-ray analysis of the PLZT sample was performed and the results were compared with infrared spectroscopy work. It was concluded that infrared optical reflectivity measurements, as a non-destructive method, can give more reliable results at the boundary cases when it is very difficult to distinguish if a material has either a cubic or tetragonal lattice structure.

1. Introduction

Lead titanate zirconate (PLZT) ceramics modified by lanthanum constitute a wide variety of compositions. They are used as piezoelectric and pyroelectric materials and are well known as high optical transparent materials with specific electro-optic properties which are used for making optical shutters and modulators, filters etc. [1]. The technology for producing PLZT ceramics with maximum transparency, and desired electro-optic properties, must be very carefully conducted. They require a special powder preparation technique and a specific sintering procedure, including hot pressing [2]. Various technological conditions must be fulfilled in order to obtain an optimal optical quality of PLZT ceramics using hot pressing.

A large amount of research work has been done in studying mechanical, structural, electrical and optical properties of PLZT. There are several papers in which their spectroscopic properties were investigated [3, 4].

In this work, far infrared and mid infrared properties of PLZT ceramics with the following composition: $\text{Pb}_{0.905}\text{La}_{0.095}(\text{Zr}_{0.65}\text{Ti}_{0.35})_{0.9725}\text{O}_3$, were examined with the intention of showing that infrared spectroscopy experiments and their analyses can give very useful information in the boundary cases when it is very difficult to find out the crystallographic properties of these perovskite materials.

2. Experimental procedure

PLZT ceramics were prepared using the mixed oxide procedure and hot pressing technique. The aim was to

obtain a composition with 9.5 at% La, 65 at% PbZrO_3 and 35 at% PbTiO_3 with the following formula: $\text{Pb}_{0.905}\text{La}_{0.095}(\text{Zr}_{0.65}\text{Ti}_{0.35})_{0.9725}\text{O}_3$ and with an excess of 3% w/o PbO, which was added in the initial batch composition in order to obtain high optical quality PLZT ceramics [1, 2]. The content of lanthanum was chosen in agreement with the phase diagram for PLZT ceramics [1, 2], which is given in Fig. 1. It shows that there is extensive solid solution of La_2O_3 in PbZrO_3 and PbTiO_3 throughout the phase diagram. It can also be seen that when the ratio of PbZrO_3 and PbTiO_3 is 65/35 an addition of 9 at% La is sufficient to reduce the stable region of the ferroelectric rhombohedral phase to below room temperature at a rate of about $37^\circ\text{C at \%}^{-1}$ La. The phase diagram shows that the boundary composition of 9.5 at% La and 65/35 ratio, of PbZrO_3 and PbTiO_3 , PLZT ceramics should have a tetragonal lattice at room temperature. Hot pressed PLZT ceramic samples were cut and polished to a thickness of about 400 μm . The samples were polished to a high optical transparency.

The crystal structure and lattice parameters of the sample were investigated using the X-ray powder method with a Phillips diffractometer. Twenty-one Bragg reflections were measured between $2\theta = 5$ and 120° , which were used to calculate the lattice parameters using the least squares method. First, these experimental data were analysed presuming that the sample had a tetragonal structure. The results obtained for the PLZT sample are given in Table I, where V_0 is the volume of the unit cell.

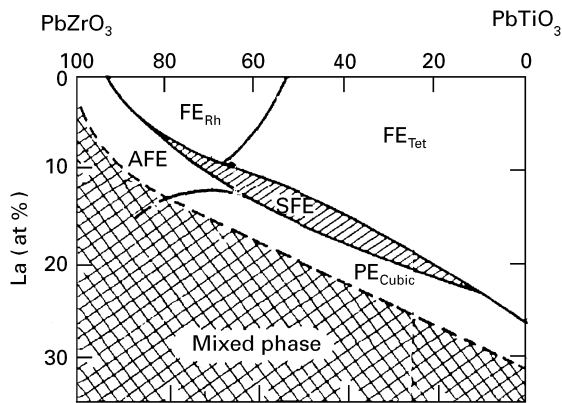


Figure 1 The phase diagram of PLZT ceramic.

TABLE I The tetragonal unit cell parameters of PLZT

PLZT sample	Tetragonal unit cell	Cubic unit cell
a_0 , nm	0.408469 ± 0.00021	0.408485 ± 0.000048
c_0 , nm	0.408795 ± 0.000052	—
V_0 , nm ³	5.8206 ± 0.00708	6.81597 ± 0.0024

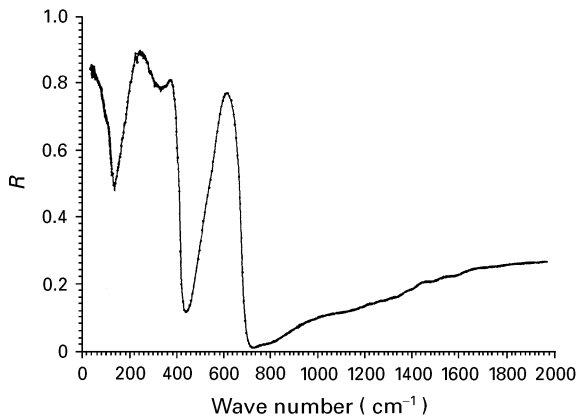


Figure 2 The reflectivity diagram, R , as a function of wave number. The experimental results are given with dots. The full curve was calculated using Kramers-Krönig analysis.

In the same table the results when the cubic structure of the sample was calculated are given. It was possible to do that because a similar crystal structure exists which belongs to a perovskite group known as tausonite, Sr-Ti oxide (JCPDS card 35-734). It is interesting to notice that the error for the presumed cubic unit cell was one order smaller for the “ a_0 ” parameter. The difference between the “ a_0 ” parameter for the tetragonal and cubic structure was ($\Delta a_0 = 0.000016$ nm), much smaller than the standard deviation error of both tetragonal or cubic parameters.

A highly polished PLZT sample was used for optical measurements. Far infrared and mid infrared reflectivity measurements for the PLZT sample were made at room temperature with a near normal incidence light using a Bruker 1130 Fourier transform infrared (FT-i.r.) spectrometer in the range 40–1500 cm^{-1} . The resolution of the measurements

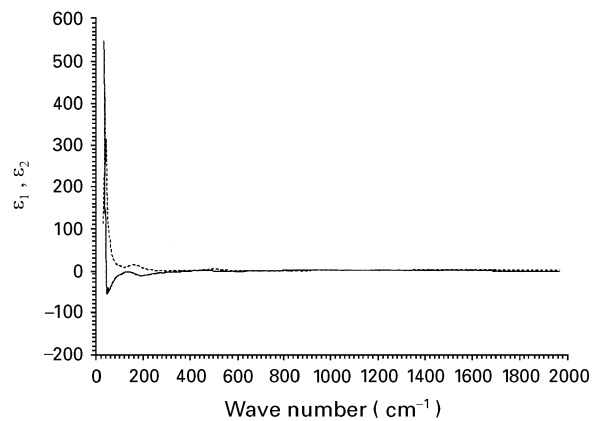


Figure 3 The real, ϵ_1 (—), and imaginary, ϵ_2 (---), parts of the complex dielectric function versus the wave number which were calculated using Kramers-Krönig analysis.

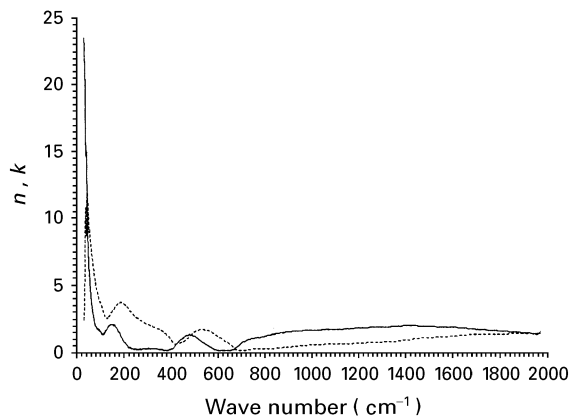


Figure 4 The refractive index, n (—), and extinction coefficient, k (---), versus the wave number which were calculated using Kramers-Krönig analysis.

was better than 1 cm^{-1} . The number of scans during these measurements was 256, therefore the signal-noise ratio for the sample and the reference mirror allowed one to conclude that the precision of the reflectivity measurements was better than 1%. The reflectivity diagram as a function of the wave number is given in Fig. 2. The experimental results are shown by dots, while the full curve was calculated using Kramers-Krönig analysis. The error bars are of the size of experimental points. The diagrams of real, ϵ_1 , and imaginary, ϵ_2 , parts of the complex dielectric function are given in Fig. 3, with a full line and a dashed curve, respectively. Fig. 4 shows the refractive index (with a full line) and the extinction coefficient (with a broken line), versus the wave number. Finally the response function, $Im(-1/\epsilon)$, versus the wave number is given in Fig. 5.

Phonon frequencies deduced from Kramers-Krönig analysis are shown in Table II, where $\omega_{j\text{TO}}$ and $\omega_{j\text{LO}}$ are transverse (TO) and longitudinal (LO) frequencies and ϵ_0 and ϵ_∞ represent the low and high frequency contribution to the dielectric parameters. The parameter ω_{TO} was deduced from peaks of the imaginary part of the dielectric function, ϵ_2 , and ω_{LO} from peaks of the response function.

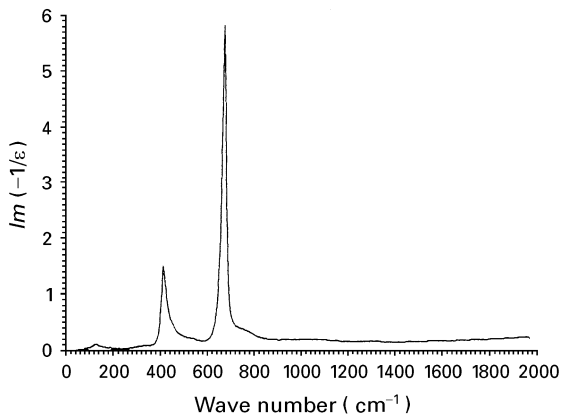


Figure 5 The response function, $Im(-1/\epsilon)$, versus the wave number which was calculated using Kramers–Krönig analysis.

Obtained experimental results were also numerically analysed using the four parameter model introduced by Gervais and Piriou [5]. The factorized form of the dielectric function is

$$\epsilon = \epsilon_1 \pm i\epsilon_2 = \epsilon_\infty \prod_i \frac{\omega_{jLO}^2 - \omega^2 + i\gamma_{jLO}\omega}{\omega_{jTO}^2 - \omega^2 + i\gamma_{jTO}\omega} \quad (1)$$

In Fig. 6 the experimental reflectivity curve (with dots) and the calculated curve obtained with this fitting procedure are given.

Table II gives the oscillator parameter and dielectric permittivity for the observed oscillators. They were deduced from a least squares computer fit to the experimental reflectivity data, where γ_{jLO} and γ_{jTO} represent the damping factor of longitudinal and transversal optical frequencies for each oscillator. These results are in reasonable agreement with the Kramers–Krönig analysis given in Table II.

The real and imaginary parts of the complex dielectric permittivity in the far infrared range for PLZT calculated with the four parameter method are given in Fig. 7, while the refractive indices (with a full line) and extinction coefficient (with a broken line), versus wave number are given in Fig. 8.

3. Discussion

It is well known that materials with a cubic perovskite structure should have three ionic oscillators and they are assigned in the literature [3] to be at about 10, 210 and 550 cm^{-1} . The fourth mode was also discussed [3] which was named a “silent F_{2n} mode of the cubic phase which is activated below critical temperature,

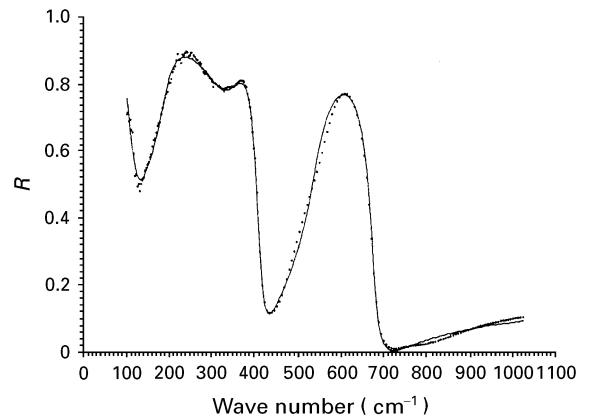


Figure 6 The experimental reflectivity diagram, R (\dots), and the calculated curve (—) obtained with the fitting procedure (four parameter model).

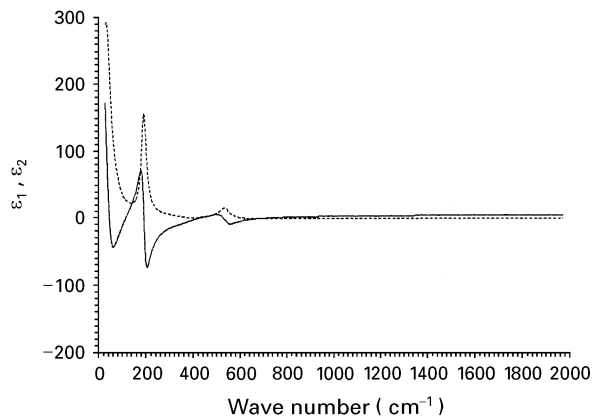


Figure 7 The real, ϵ_1 (—), and imaginary, ϵ_2 (---), parts of the complex dielectric function versus the wave number which were calculated using the four parameter model.

T_c ”. It is also known that at the temperature, T_c , the unit cell of PLZT changes from a cubic (with space group P_{m3m}) to a tetragonal structure (with space group $P4_{mm}$). The number of infrared active modes for both crystal unit cells was calculated using group theory analysis and Adams–Newton tables [6]. For a cubic cell and the space group P_{m3m} there are only $3F_{1n}$ active vibrational modes, while for the $P4_{mm}$ space group there are eight active modes: $4A_1 + 4E$ (parallel to the c -axis or normal to it, respectively). That means that for a tetragonal structure there are eight infrared active vibrational modes. All these modes can be observed if they are strong enough.

When optical properties of a polycrystalline PLZT sample were measured four infrared oscillators were

TABLE II Phonon frequencies (in cm^{-1}) deduced from Kramers–Krönig analysis and the four parameter model

Kramers–Krönig				Number of oscillators	Four parameters fit				ϵ_0	ϵ_∞
ϵ_0	ϵ_∞	ω_{TO}	ω_{LO}		ω_{TO}	ω_{LO}	γ_{TO}	γ_{LO}		
230	5.0	43.4	122.4	1	42.0	126.4	54.7	48.5	5.17	
		188.5	355.0	2	187.2	357.4	20.9	188.0		
		353.0	408.0	3	358.0	408.0	111.0	32.7		
		525.0	656.0	4	526.0	660.5	43.2	34.8		

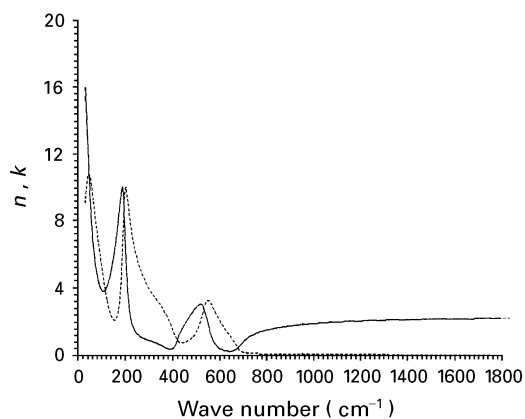


Figure 8 The refractive index, n (—), and extinction coefficient, k (---), versus the wave number which were calculated using the four parameter model.

observed, which are given in Table II. One could say that even a fifth mode is practically visible at about 100 cm^{-1} where some sort of a knee exists in the reflectivity diagrams given in Fig. 2 and Fig. 6. This shows that there is at least one more oscillator for PLZT at room temperature compared with the cubic perovskite unit cell. Only this statement is enough to prove that the unit cell cannot be cubic. For a complete infrared analysis one needs to have a single crystal PLZT sample. In the present case, only a high quality polycrystalline sample was available. In this case one cannot distinguish if the oscillator belongs to $E \perp c$ or $E \parallel c$ of a tetragonal unit cell. But still, one surely can say that one has observed more than three oscillators judging by Figs 3 and 7, and especially Figs 4 and 8. In Fig. 3 three peaks for ϵ_2 between 30 and 400 cm^{-1} were identified. The fourth peak is better exposed in Fig. 7 (at about 520 cm^{-1}). Figs 4 and 8 represent the index of refraction and extinction coefficient versus the wave number obtained with the Kramers–Krönig or four parameter method, respectively. In both figures the existence of four oscillators is obvious.

The oscillator energy, E_{osc} , was also calculated for each oscillator using the following equation

$$E_{\text{osc}} = \epsilon_{2\text{max}} \gamma_{\text{TO}} \omega_{\text{TO}} \quad (2)$$

The ratio between the oscillator energy with the highest and lowest energy is, $E_{\text{osc}3}/E_{\text{osc}1} \approx 4.6$. It may

be expected that if measurements were made at the liquid helium temperature oscillators with a very high energy could be observed as two or more individual oscillators.

4. Conclusions

In this work it was investigated and confirmed that infrared optical reflectivity measurements and numerical analysis can be successfully used for obtaining reliable information about whether a sample has a cubic or tetragonal unit cell. That is very important especially for materials with a perovskite lattice in situations where it is very difficult to solve this problem using only X-ray work. An example of this case is demonstrated in this work.

Acknowledgements

This work is part of the research activity carried out through projects: “Prognosis of Materials Properties” and “Physical Chemistry Processes in the Technology of Advanced Materials”. The authors would like to express their gratitude to the Serbian Academy of Sciences and Arts and to the Science Council of the Republic of Serbia for their financial support. We would specially like to thank V. Poharc-Logar and V. Blagojević for their help during our work on this paper.

References

1. G. H. HEARTLING, *Ferroelectrics* **75** (1987) 25.
2. B. D. STOJANOVIĆ, M. KOSEC and D. KOLAR, *J. Serb. Chem. Soc.* **59(a)** (1994) 655.
3. V. ŽELEZNY, P. SIMON and F. GERVAIS, *Mater. Res. Bull.* **22** (1987) 1695.
4. V. ŽELEZNY, J. PETZELT, A. A. VOLKOV and M. OZOLYINSH, *Ferroelectrics* **109** (1990) 149.
5. F. GERVAIS and B. PIRLOU, *Phys. Rev. B* **10** (1974) 1642.
6. D. M. ADAMS and D. C. NEWTON, “Tables for Factor Group and Point Group Analysis” (Bedeman, RIIC, 1970).

Received 22 February
and accepted 17 July 1995